

TECHNICAL NOTE

Chemical Characterization in the Production Chain of Permanent Magnets by Inductively Coupled Plasma Optical Emission Spectrometry (ICP OES)

Precise Quantification of Nd, Pr, Fe and B in Super-Magnets Samples

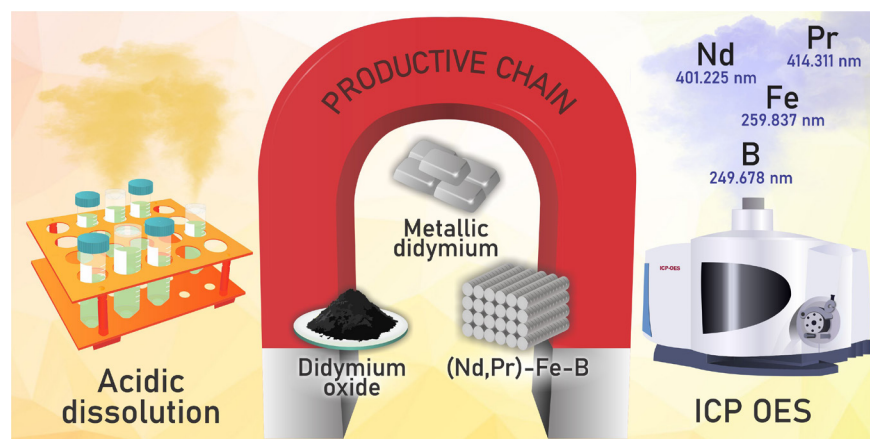
Rodrigo Papai*¹, Karina Torre da Fonseca², Gilmar Alves de Almeida^{1,3}, André Luiz Nunis da Silva¹, Thiago Pires Nagasima¹, Eduardo Gimenes Jabes^{1,4}, Célia Aparecida Lino dos Santos¹, Fernando José Gomes Landgraf⁴, Maciel Santos Luz*¹

¹Instituto de Pesquisas Tecnológicas do Estado de São Paulo (IPT), Avenida Professor Almeida Prado, 732, Cidade Universitária, 05508-901, São Paulo, SP, Brazil

²Instituto de Química da Universidade de São Paulo (IQ USP), Avenida Professor Lineu Prestes, 748, Cidade Universitária, 05508-000, São Paulo, SP, Brazil

³Instituto de Pesquisas Energéticas e Nucleares (IPEN), Avenida Professor Lineu Prestes, 2242, Cidade Universitária, 05508-000, São Paulo, SP, Brazil

⁴Escola Politécnica da Universidade de São Paulo (EP USP), Avenida Professor Luciano Gualberto, 380, Cidade Universitária, 05508-010, São Paulo, SP, Brazil



Super-magnets, materials whose strong magnetic activity is an attractive differential for the high-tech industry, may have their magnetic performance affected by small variations in their chemical composition. For example, the neodymium and praseodymium content can change the physicochemical properties of the permanent magnets. Aiming at a strict chemical quality control, this work developed an analytical

method to quantify the major elements in the materials involved in the production process of didymium (the mixture of neodymium and praseodymium) super-magnets. The simultaneous determination of Nd (401.225 nm), Pr (414.311 nm), Fe (259.837 nm) and B (249.678 nm) in three different sample types (didymium oxide, metallic didymium and (Nd,Pr)-Fe-B alloy) was performed by sample dissolution in acidic media, followed by instrumental measurements using an Inductively Coupled Plasma Optical Emission

Cite: Papai, R.; da Fonseca, K. T.; de Almeida, G. A.; da Silva, A. L. N.; Nagasima, T. P.; Jabes, E. G.; dos Santos, C. A. L.; Landgraf, F. J. G.; Luz, M. S. Chemical Characterization in the Production Chain of Permanent Magnets by Inductively Coupled Plasma Optical Emission Spectrometry (ICP OES) – Precise Quantification of Nd, Pr, Fe and B in Super-Magnets Samples. *Braz. J. Anal. Chem.* 2022, 9 (36), pp 124–145. <http://dx.doi.org/10.30744/brjac.2179-3425.TN-108-2021>

Submitted 21 October 2021, Resubmitted 01 April 2022, Accepted 15 April 2022, Available online 17 May 2022.

Spectrometer. Linear calibration curves were obtained with high coefficient of determination ($0.9983 \leq R^2 \leq 0.9999$) and with appropriate limits for determining these elements at the percentage level, reaching detection limits less than 0.07 cg g^{-1} . The precision of the method was improved by weighing of the solutions during all the dilution steps and was evaluated by the coefficient of variation associated to instrumental precision (0.3 – 0.7%), method intermediate precision (1.9 – 3.1%) and also by the typical mass fraction provided as uncertainty ($0.04 - 0.20 \text{ cg g}^{-1}$), reaching the pressing need to distinguish the content of the rare earth elements in less than 1 cg g^{-1} . The accuracy of the method was assessed by spiked and recovery test (96-104% for spikes equal to or greater than 0.50 cg g^{-1}) and also by the use of different analytical methods, involving the participation of other laboratories, obtaining an acceptable degree of agreement (85 – 107%).

Keywords: Didymium magnets, ICP OES, (Nd,Pr)-Fe-B

INTRODUCTION

Present in electric motors, wind turbines and data storage devices (hard disk), magnets are indispensable in the manufacture of computers, televisions, cell phones, smart watches and other various modern electronic devices.^{1,2} The chemical composition of the magnet directly influences its magnetic performance with a consequent impact on the quality of the associated products.³⁻⁶ In this context, knowing the major chemical composition of magnets contributes to a more efficient quality control in the act of production and also helps manufacturers in the high-tech industry to select magnets in order to keep the uniformity of these materials, valuing the isonomy of the final products with higher added value.

Although there are several magnet types, those that employ rare earth elements (REE) generally have strong magnetic activity,^{1,7-11} and are often called permanent magnets or super-magnets.^{2,3} Among the REE, the mixture of neodymium and praseodymium (called didymium^{12,13}) is widely used in metal alloys together with the elements iron and boron to act as a super-magnet. Currently, the most powerful commercial magnets used in the world employ neodymium¹⁴ or didymium.¹⁵⁻¹⁸

The production chain of metal alloy (Nd,Pr)-Fe-B is briefly summarized into the following steps: (i) in the production of didymium oxide (a mixture of neodymium and praseodymium oxides) through a process of separation of the ore that contains REE; (ii) the electrolytic reduction of didymium oxide, in order to obtain metallic didymium (a solid solution containing neodymium and praseodymium) and (iii) the incorporation of elemental iron and boron in the metallic didymium in liquid phase (process carried out under high temperatures) to finally obtain the metallic alloy (Nd,Pr)-Fe-B. The chemical composition of the super-magnets varies according to the application. In general, the typical contents of the elements in this alloy ranged around $25\text{-}35 \text{ cg g}^{-1}$ of didymium, $0.5\text{-}2.0 \text{ cg g}^{-1}$ of boron and $60\text{-}75 \text{ cg g}^{-1}$ of iron. According to the need for the application, other minority elements can be added.¹⁹

After the production of the metal alloy, the magnet can be obtained by several processes that involve: hydrogen embrittlement (or also called hydrogen decrepitation²⁰⁻²²); milling;²³ magnetic particle alignment, which is induced by an intense magnetic field applied under the material; compaction; sintering and appropriate heat treatments, thus giving rise to the super-magnet.

In order to reduce cost, the chemical composition must minimize the use of REE. However, the reduction of REE content may cause alpha iron phase (an allotrope of iron with a body-centered cubic crystalline structure) to be present in magnets, which has a negative effect on the desired magnetic properties of the super-magnet and hinders further processing steps, such as the hydration and sintering of the alloy.²⁴

Small variations in the Nd and Pr content strongly influence the physicochemical properties of the alloy, for this reason studies about alloy development involve minimal variations in the REE content. In this way, the chemical characterization of the alloy and the main materials involved in its production process are important to achieve the desired properties in these magnetic materials. Therefore, chemical analytical methods must be able to distinguish small variations in the concentration of their constituent elements.

Among the analytical techniques of elemental determination, those that allow direct solid analysis, would be ideal for analysing such materials, mainly due to: (i) high analytical frequency, which allows fast analysis of solid materials; (ii) the practicality of minimizing the sample treatment step or even eliminating it and (iii) the reduction of possible errors inherent in sample handling.²⁵ Currently, the main techniques for direct solids analysis include: Laser-Induced Breakdown Spectroscopy (LIBS),²⁶⁻³⁰ X-ray Fluorescence (XRF),³¹⁻³³ Laser Ablation Inductively Coupled Plasma Mass Spectrometry (LA-ICP-MS),^{34,35} Graphite Furnace Atomic Absorption Spectrometry (GF AAS),³⁶ among others.²⁵

However, to quantify the analytes most of these techniques require calibrating materials, that is, solid standards whose chemical composition is well known with a suitable degree of accuracy and precision in a similar matrix to the sample. Unfortunately, to date, such solid standards for the materials involved in the production process of super-magnets are not available.

Considering the unavailability of calibrating materials for use in direct analysis of solids and aiming at a reliable analytical method to quantify Nd, Pr, Fe and B simultaneously in three different types of samples involved in production process of super-magnets (didymium oxide, metallic didymium and (Nd,Pr)-Fe-B alloy), this work reports the synthesis of these materials and a simple protocol for the dissolution of the sample in diluted acid solutions and subsequent quantification of analytes by Inductively Coupled Plasma Optical Emission Spectrometry (ICP OES), an instrumental technique with great potential for reliable determination of rare earth elements.^{3,37-39}

The determination of chemical elements in samples of permanent magnets based on rare earths by ICP OES is not new, and it is possible to find old articles that mention having performed elemental analysis by ICP. However, the description of how to proceed with this chemical measurement task in these samples is scarce in the literature. In a world in which the reliability of the results is increasingly necessary, this work contributes with a detailed account of a robust method, which provides precise and accurate results. For the first time, a complete analytical method is reported to determine the main elements in the production chain of didymium permanent magnets. With the intention of establishing a standard method to be implemented routinely, the novelty of this work is centered on meeting the quality criteria necessary in the production chain of didymium magnets and it stands out for the: (i) high reliability of the results, (ii) high precision obtained, which allows to distinguish low contents of rare earth elements and (iii) in the evaluation of foreign elements that can be potential interfering species, making this paper act as a guide for the development of analytical applications in similar samples.

MATERIALS AND METHODS

Reagents and solutions

Standard solutions of neodymium $100,434 \pm 450 \text{ mg L}^{-1}$ (Specsol™), praseodymium $100,497 \pm 450 \text{ mg L}^{-1}$ (Specsol™), iron $10,027 \pm 50 \text{ mg L}^{-1}$ (SPEX CertiPrep™) and boron $1,002 \pm 4 \text{ mg L}^{-1}$ (SCP Science™) were used as reference solutions for calibration by external standardization.

Neodymium and praseodymium oxides were purchased from HEFA Rare Earth Canada Co.Ltd.™

Nitric acid solution 25% (v/v) was prepared by the slow addition of 25 mL of concentrated acid (65% w/w, Merck™) in 75 mL of deionized water.

Hydrochloric acid solution 27% (v/v) was prepared by the slow addition of 27 mL of concentrated acid (37% w/w, Merck™) in 73 mL of deionized water.

Samples and preparation

Three different sample types related to permanent magnets manufacturing process were evaluated in this study: (i) didymium oxide, obtained by mixing praseodymium and neodymium oxides; (ii) metallic didymium (solid solution containing Nd and Pr), produced in our laboratory by igneous electrolytic reduction, using molten lithium fluoride and didymium oxide concentrate and (iii) (Nd,Pr)-Fe-B alloy, prepared with the previously produced metallic didymium by the incorporation of iron and boron elements in liquid phase, followed by solidification and subsequent strip casting procedure. The samples were stored in an inert

atmosphere (argon gas) to prevent oxidation⁴⁰ and were exposed to atmospheric air only seconds before the sample treatment (acid dissolution).

The subsamples were divided in three different test portions ($n = 3$). Each test portion was weighed directly in a conical polypropylene tube (Falcon, Corning™) with a capacity of 50 mL until reaching a mass ideally close to the following values: 0.3, 0.4 and 0.5 g for didymium oxide, metallic didymium and (Nd,Pr)-Fe-B alloy sample, respectively. The real mass value was recorded (considering up to 4 decimal places) and then the samples dissolution was started.

In a fume hood, the dissolution of metallic didymium and (Nd,Pr)-Fe-B alloy samples was carried out in acidic solutions, containing 15 mL of nitric acid (25% v/v) and 5 mL of hydrochloric acid (27% v/v) for each test portion. Also in a fume hood, the didymium oxide was dissolved with 10 mL of concentrated hydrochloric acid (37% w/w) and 10 mL of concentrated nitric acid (65% w/w) until the dissolution reaction was completed (obtained visually when reaching a translucent colour).

When necessary, in exceptional cases, increments of up to 4 mL of concentrated nitric acid (65% w/w) were added, until the dissolution reaction was completed (obtained visually when reaching a translucent colour).

The initial mass of each tube was recorded and then after the dissolution step, the volume was completed to 50 mL with deionized water. Next, the final dissolved sample was weighed and its mass was recorded to calculate the real dilution factor. Using a micropipette and also weighing on the analytical balance, the resulting solution (sample dissolved) was diluted by factors of 150, 200 or 250-fold for (Nd,Pr)-Fe-B alloy, didymium oxide and metallic didymium, respectively, prior to analysis.

Blank solutions were prepared by adding all the reagents described previously without the samples. All solutions were produced in triplicate ($n = 3$).

ICP OES instrumentation and conditions

Inductively Coupled Plasma Optical Emission Spectrometer (iCap 7400 Duo, Thermo Scientific™) was used for chemical analysis. The main conditions used during the ICP OES analysis, such as: (i) nebulizer gas flow, (ii) RF generator power, (iii) peristaltic pump frequency and (iv) argon auxiliary gas flow were optimized, aiming to achieve the highest signal-to-background ratio, with 14 different parameters sets being evaluated. The optimal conditions are summarized in Table I.

Table I. Operational conditions optimized for ICP OES analysis

Parameter	Condition
RF generator power	27.12 MHz solid state, operated at 1150 W
Coolant gas flow rate (argon)	12 L min ⁻¹
Auxiliary gas flow rate (argon)	0.50 L min ⁻¹
Nebulizer type	Concentric (glass)
Spray chamber	Glass Cyclonic
Nebulizer gas flow	0.50 L min ⁻¹
Sample flow rate	1.55 mL min ⁻¹ (50 rpm)
View mode	Axial
Exposure time	15 s for UV and 5 s for Visible measurements
Replicates	3
Monitored analytical lines	Nd II 401.225 nm Pr II 414.311 nm Fe II 259.837 nm B I 249.678 nm

Calibration

Calibration curves were constructed with 10 points by diluted standard solutions containing the analytes together in the range of 10.0 to 32.5 mg L⁻¹ for neodymium, 0.10 to 10.00 mg L⁻¹ for praseodymium, 30 to 57 mg L⁻¹ for iron and 0.1 to 1.8 mg L⁻¹ for boron. All dilutions were properly weighed using the analytical balance, recording the mass of each concentrated standard added to calculate the concentration of the solution accurately.

RESULTS AND DISCUSSION

The main results and the parameters that characterize an analytical method are discussed throughout the article, emphasizing: (i) Sample dissolution; (ii) Optical measurements and pixel selection; (iii) Calibration and limits of detection and quantitation; (iv) Precision; (v) Accuracy; (vi) Foreign elements and interference evaluation and (vii) Comparative analytical methods, advantages and drawbacks.

Sample dissolution

The complete dissolution of the sample was easily reached with the combination of nitric and hydrochloric acid, due to its oxidation strength. The concentrations reported in the experimental section were optimized to allow a quick and safe dissolution. Since both the metallic didymium and the (Nd,Pr)-Fe-B alloy can react violently with the acid mixture, the need to use diluted acids to prevent the release of particles was noticed. In contrast, didymium oxide exhibited less reactivity and therefore, its dissolution was affected with concentrated acids in a longer time (more than 1 hour). Visual observation indicated that heating in a water bath around 90 °C can accelerate the sample dissolution time by up to 70%.

Although sample treatment is not such a difficult step, the analytes determination by optical spectrometry poses some challenges. For example, the high similarity in the electronic structure between the atoms of Nd and Pr can cause intense spectral interferences. This requires the use of a high resolution spectrometer, that is capable of resolving these interferences or the use of interference correction strategies.³ The high amount of iron in the sample is also a challenge, as this is a chemical element known to emit at different wavelengths. Therefore, there is also a need to select appropriate wavelengths for measurement, as well as to control the content of Fe injected into ICP OES instrument.

Optical measurements and pixels selection

All optical emission measurements were performed in axial view. Although the instrument allows measurements in radial view, less sensitivity was obtained in this condition, making it difficult to distinguish between small concentrations of the analytes in solution. Tests performed with radial measurements required a lower sample dilution factor and, consequently, higher concentrations of the standards in the calibration curve to obtain appreciable emission intensities. However, in this condition, the greater number of chemical species introduced into ICP OES instrument caused wear of the torch, accumulating a thin metallic film on the quartz surface, that hinders the constancy of the plasma and consequently affected the long-term stability. Therefore, aiming to keep the analytical performance characteristics stable for a long time of operation and also aiming at a longer torch durability, the axial view measurement mode was chosen.

Different wavelengths were evaluated for quantitative measurements of Nd (378.425; 386.341; 401.225; 406.109; 415.608; 430.358 and 489.693 nm), Pr (390.844; 414.311; 417.939; 422.535 and 495.137 nm), Fe (233.280; 234.349; 238.204; 239.562; 240.488; 259.837; 261.187 and 371.994 nm) and B (181.837; 182.591; 182.641; 208.893; 208.959; 249.678 and 249.773 nm). Aiming at high precision quantifications, the best wavelengths were chosen based on: (i) greater intensity obtained in the central pixels; (ii) lower background observed to the right and left pixels of the emission peak and (iii) lower relative standard deviation of replicate measurements (n = 3). Thus, based on these criteria, the wavelengths selected for the quantification of Nd, Pr, Fe and B were 401.225, 414.311, 259.837 and 249.678 nm, respectively.

The emission spectra of the selected wavelengths are shown for a set of calibration solutions in the Figure 1. The spectra recorded for the dissolved samples exhibited the same peak shape.

To guarantee the absence of spectral interference mono-elemental standards were analysed independently. The results of the emission intensities allowed the calibration with multi-elemental solutions, without any spectral interference.

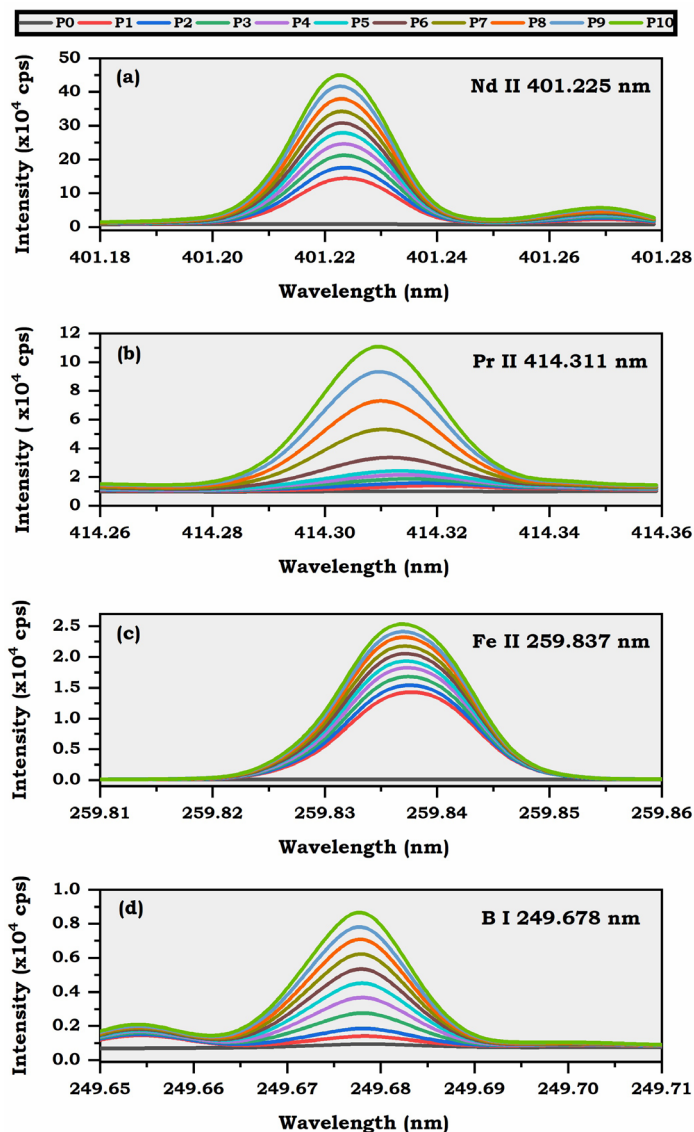


Figure 1. Fragment spectra obtained by ICP OES with standard solutions from blank (P0) to high calibration standard (P10), showing the peak emission for analytes.

According to Figure 1, for the Nd quantification, central pixels corresponding to the range of 401.217 – 401.233 nm were selected and lateral pixels for subtracting the background in the ranges of 401.176 – 401.183 nm (left) and 401.250 – 401.257 nm (right). For Pr quantification, central pixels located between 414.304 – 414.320 nm and lateral pixels at 414.262 – 414.269 nm (left) and 414.347 – 414.355 nm (right) were used. The quantification of Fe involved the pixels at 259.833 – 259.843 nm (central), 259.801 – 259.806 nm (left) and 259.865 – 259.870 nm (right). Boron utilized the following selected pixels: 249.672 – 249.682 nm (central) and 249.708 – 249.713 nm (right), without pixels selected on the left, since residual emissions occur on the left side close to the emission peak, due to weak Fe I 249.653 nm emission line.

Calibration and limits

Linear responses between the emission intensity and the analyte concentration were obtained, according to linear regression by the method of least squares. The proper linear fit was confirmed by the high coefficient of determination ($0.9983 \leq R^2 \leq 0.9999$) and also by the random distribution in the residual plots, with less than 4% of bias at each calibration point, as seen in Figure 2. The main parameters, such as calibration sensitivity, coefficient of determination and explored linear range are shown in Table II.

Although new calibration approaches⁴¹⁻⁴⁴ are available, the external calibration with standard solutions was chosen in this work due to the high similarity of the aqueous standards with the diluted aqueous samples (whose composition is mostly Nd, Pr, Fe and B dissolved in acidic media). The acid concentration of the standards was matched with the final acid concentration of the sample (after dilution), to eliminate possible matrix differences.

The lower limit of detection (LLOD) was reported in two ways: Instrument detection limit (IDL) and method detection limit (MDL). The IDL refers to the smallest amount of analyte needed to obtain a signal significantly different from the blank in ICP OES, this limit was statistically estimated based on the standard deviation of 10 consecutive measurements from a blank solution (s_B) and considering the calibration sensitivity (m) at 98.3% confidence level⁴⁵, such that: $IDL = 3 \times s_B/m$. The IDL values ranged from 0.009 to 0.028 mg L⁻¹ and were reported in Table II. Additionally, the MDL considers all dilution steps involved in the analytical sequence, providing the minimum detectable amount of analyte as a function of the sample mass. The BEC values reported in Table II are equivalent to the average value of nine points calculated at different levels of analyte concentration, ranging from 0.011 to 0.044 mg L⁻¹. For all analytes, the concentration required to exhibit the same intensity as the background proved to be below the instrumental quantitation limit (IQL), this rule out possible errors induced by the background in the instrumental measurements within the established limits.

Table II. Instrumental analytical performance characteristics in aqueous solution

Analyte	Calibration sensitivity ^a (cps L mg ⁻¹)	R ²	Exploited linear range (mg L ⁻¹)	IDL (mg L ⁻¹)	IQL (mg L ⁻¹)	BEC (mg L ⁻¹)
Nd	$1.4(\pm 0.3) \times 10^{-4}$	0.9999	10.0 – 32.5	0.022	0.073	0.011
Pr	$9.3(\pm 0.2) \times 10^{-3}$	0.9994	0.1 – 10.0	0.009	0.030	0.019
Fe	$4.0(\pm 0.2) \times 10^{-3}$	0.9983	30.0 – 57.0	0.026	0.086	0.010
B	$3.1(\pm 0.4) \times 10^{-3}$	0.9990	0.1 – 1.8	0.028	0.092	0.044

^aSlope values with standard deviation for 10 calibration curves obtained on different days.

Table III shows MDL values for the three different sample types and these limits were below 0.07 cg g⁻¹, these values fully satisfy the conditions for quantitative chemical analysis of the samples evaluated in this study. Eventually, if necessary, lower MDL values can be achieved by decreasing the dilution factor of the samples employed by this method.

Analogously, the lower limit of quantitation (LLOQ) was reported by the instrumental quantitation limit (IQL), ranging from 0.030 to 0.092 mg L⁻¹ and also by the practical quantitation limit (PQL), ranging from 0.03 to 0.25 cg g⁻¹. These limits refer to the lowest analyte concentration that can be measured with reasonable accuracy in aqueous solutions (IQL) and by the proposed method, covering all dilutions steps (PQL). Both, IQL and PQL, were estimated as 10/3 x IDL and MDL, respectively.

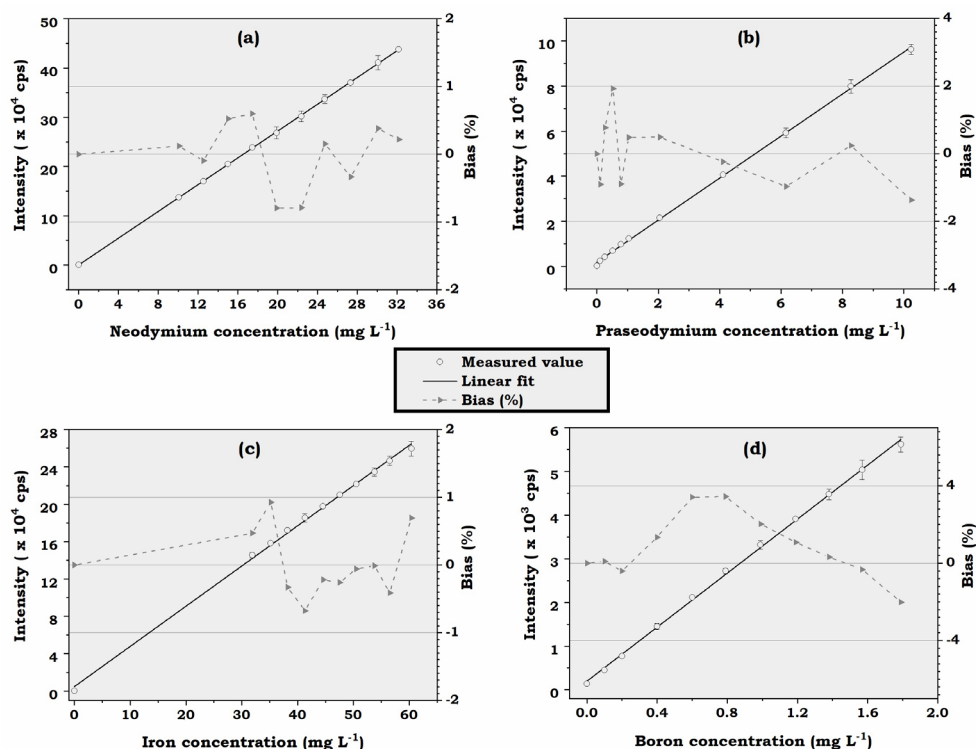


Figure 2. Calibration curves for (a) Neodymium, (b) Praseodymium, (c) Iron and (d) Boron obtained in ultrapure water containing 2% w/v of nitric acid. The graphs show the intensities in the left y-axis and the percentage bias in the right y-axis. Vertical error bars refer to ± 1 standard deviation of triplicate measurements ($n = 3$).

All analytical signals were measured in the presence of some degree of background, which can be originated from the emission from the plasma and also due to the detector and electronic characteristics. To assess the extent of this effect, the background equivalent concentration (BEC) was estimated for each wavelength used in analytical measurements by the following equation: $BEC = (C_{std} \times I_B) / (I_{std} - I_B)$, where C_{std} is the concentration of a standard solution, I_{std} is the emission intensity measured for the same standard solution and I_B is the intensity of the blank solution. The BEC values ranging from 0.011 to 0.044 mg L⁻¹, reported in Table III are equivalent to the average value of nine points calculated at different levels of analyte concentration. For all analytes, the concentration required to exhibit the same intensity as the background proved to be below the instrumental quantitation limit (IQL), this rule out possible errors induced by the background in the instrumental measurements within the established limits.

Table III. Figures of merit for different sample types

Sample type	Analyte	MDL (cg g ⁻¹)	PQL (cg g ⁻¹)	Mass fraction covered by calibration (cg g ⁻¹)
Didymium oxide	Nd	0.07	0.25	33.00 – 100.00
	Pr	0.03	0.09	0.33 – 33.00
Metallic Didymium	Nd	0.07	0.25	31.25 – 100.00
	Pr	0.03	0.09	0.31 – 31.25
(Nd,Pr)-Fe-B alloy	Nd	0.03	0.09	15.00 – 48.75
	Pr	0.01	0.03	0.15 – 15.00
	Fe	0.05	0.17	45.00 – 85.50
	B	0.04	0.13	0.15 – 2.70

Precision

The precision of the results provided by the proposed analytical method was evaluated and improved in order to obtain results with the least uncertainty possible. The samples related to the production chain of super-magnets requires precise quantifications, especially for the REE. Uncertainties greater than 1 cg g⁻¹ in the mass fraction of the neodymium or the praseodymium can strongly impact the performance of permanent magnets.

Despite the instrumental precision of ICP OES (estimated by successive measurements of a standard solution performed in the same condition and on the same day) show a low relative standard deviation (RSD) ranging from 0.3 to 0.7% (as seen in Table IV), the precision of the method was initially out of the desirable, providing mass fraction results with more than 1 cg g⁻¹ of uncertainty for the neodymium and praseodymium elements. Although this uncertainty is suitable for most analytical applications, it implies difficulties in the strict quality control of the super-magnets. In order to reduce this uncertainty, the sample dilution steps applied during the execution of the method were controlled by weighing.

Traditionally, the adjusting the volume in the solutions is a routine practice in chemistry laboratories, being performed visually by the analyst, who has the task of controlling the amount added until the liquid reaches the meniscus mark in precision glassware. In this practice, the volume adjustment is subject to intrinsic deviations, often insignificant for chemical analysis. However, the propagation of this uncertainty inevitably occurs in the method. To minimize the uncertainties arising from the dissolution and dilution of the samples, the solutions were weighed on an analytical balance and the recorded masses were used to calculate the dilution factor. Although the sample treatment procedure becomes slower, due to the additional step of registering all the masses added for each tube, the results were more precise.

The lower uncertainties in analytes mass fraction results were reached due to the fact that the analytical balance is one of the most precise and accurate instruments in a chemical laboratory, reaching legibility up to four decimal places. Next, the control of the dilution by weighing was applied for all samples and also for the calibration solutions.

After minimizing the uncertainty associated with the sample preparation by weighing strategy, the method intermediate precision^{46,47} was assessed by the relative standard deviation (RSD) from the ten measurements of the emission intensity obtained with a specific standard solution, prepared and analysed on different days by different operators in different locations within the laboratory, using different calibration curves and the same instrument (ICP OES). The standard solution containing 42.0 mg L⁻¹ of Nd, 1.0 mg L⁻¹ of Pr, 42.0 mg L⁻¹ of Fe and 0.8 mg L⁻¹ of B was strategically selected to faithfully evaluate the method intermediate precision, since these concentrations are located in the middle of the linear ranges used for calibration curves of the proposed method. It is well known that precision is intrinsically associated with the level of analyte concentration,⁴⁸ with a systematic increase in the relative standard deviation occurring as the analyte concentration decreases.^{49,50} For this reason, the evaluation of the method precision in its extreme conditions of the linear range may not reliably represent the expected precision for most samples, which ideally are located in the middle of the linear range, especially when the method is well delineated. The method intermediate precision values are shown in Table IV and range from 1.4 to 3.1%, showing acceptable RSD values, that indicate a relative ease of the method reproduction.

In addition to the method intermediate precision, the typical uncertainty obtained for each analyte in mass fraction results (cg g⁻¹) was estimated based on the average of the uncertainties obtained for a representative set of samples (n = 80), since it is an average value, eventually some samples may deviate from the typical uncertainty reported in Table IV.

So, the minimum and maximum values of uncertainty obtained with the proposed method for that same set of samples are also shown in Table IV. It is worth mentioning that the uncertainty values in mass fractions were expressed by the standard deviation obtained in triplicate (n = 3) and do not consider a confidence interval. Table IV summarizes the main parameters related to precision.

Table IV. Precision assessment to characterize the analytical method and typical values of uncertainty obtained when applying the proposed method in real samples

Analyte	Instrumental Precision ^a	Method intermediate precision ^b	Mass fraction typical uncertainty ^c (cg g ⁻¹)	Mass fraction range uncertainty ^d (cg g ⁻¹)
Nd	0.3%	2.0%	0.20	0.03 – 0.65
Pr	0.7%	3.1%	0.07	0.01 – 0.39
Fe	0.6%	1.4%	0.69	0.02 – 2.54
B	0.6%	1.9%	0.04	0.01 – 0.20

^a Relative Standard Deviation (RSD) for 10 consecutive measurements of standard solution in the same day.

^b RSD for 10 measurements of standard solution in different days, by different analysts.

^c Average of mass fraction uncertainty for 80 samples. Typical uncertainty obtained for samples containing 16-80 cg g⁻¹ of Nd, 1-26 cg g⁻¹ of Pr, 63-70 cg g⁻¹ of Fe and 0-2 cg g⁻¹ of B.

^d Minimum and maximum value of mass fraction uncertainty obtained in final results for 80 samples.

Accuracy

Due to the absence of super-magnet reference materials, the accuracy of the method was evaluated in two different ways: (i) by spike analyte and recovery test on the three different sample types and (ii) by the comparison of the mass fraction results obtained by proposed method with other laboratories results, that applied independent analytical methods to determination a same set of (Nd,Pr)-Fe-B alloy samples. The Table V shows the spiked value and recovery percentage of the analytes at six different concentration levels. As the spike was performed on the diluted sample, the sum of the analyte concentrations may eventually be greater than 100 cg g⁻¹. Spikes equal to or greater than 0.50 cg g⁻¹ exhibited acceptable recovery values, ranging from 96 to 104% for all elements. This recovery values attests to the accuracy of the method when applied to these matrices. In smaller spikes concentrations (<0.50 cg g⁻¹), recovery values ranged from 90 to 140%, which indicates a difficulty of the method in distinguishing concentrations below 0.50 cg g⁻¹, especially for Nd, Pr and Fe. It should be noted that the quantification of boron was an exception, being able to distinguish contents on the order of 0.05 cg g⁻¹. Although some recovery values at 0.05 and 0.10 cg g⁻¹ for Nd, Pr and Fe were suitable for chemical analysis, it is observed that the uncertainty obtained is equal to or greater than the spiked concentration value, making it impossible to distinguish between those levels. Better recoveries values (96 - 104%) were obtained when considering only spikes from 0.50 cg g⁻¹.

For comparison purposes, three samples of (Nd,Pr)-Fe-B alloy (labelled A, B and C) with distinct neodymium and praseodymium content, were selected, fractionated and sent to two different chemistry laboratories, located in different countries, which applied independent analytical methods to determine the main chemical elements. The mass fraction values reported by the invited laboratories were compared with the values obtained from the proposed method by a hypothesis test (student t-test) at 95% of confidence level. Table VI shows the statistical comparison that for most determinations there was no statistically significant difference, this indicates a good agreement between the results from the proposed method and those from the invited laboratories. Small differences exist only for the guest laboratory identified by the number two (2) that reported the boron element with values statistically different from the others for samples A and C, whose calculated t-values (3.56 and 3.55, respectively) were higher than the critical t-value (2.78) at 95% confidence level. This small statistical difference reveals a peculiar characteristic for boron, whose quantification requires some additional care in relation to the other analytes.

In our laboratory, during method development, we noticed oscillations in the blank intensities for boron. A fact that eventually impaired the good linear adjustment of the calibration curves and could influence inexact quantification for this element. The intensity oscillation was investigated and was shown to be linked to: (i) the purging time with argon required for measurements in the UV range in our ICP OES

equipment and (ii) the sample introduction system, including the nebulizer, nebulization chamber and the connection to the base of the torch, which are materials made of borosilicate glass that can eventually release the boron element and introduce it into the plasma, causing oscillations in the measurement steps (especially if the sample contains fluoride in an acid medium). Both situations were solved by adopting two simple procedures, which are strongly recommended if this method is implemented in the routine of other laboratories: (i) a minimum of four hours purging optics with argon gas prior to ICP OES measurements and (ii) washing the sample introduction system with nitric acid solution (10% v/v) followed by abundant rinsing with deionized water before instrumental analysis. Despite this small difference for boron, the other results are in full agreement and demonstrate a high level of accuracy achieved with the proposed method.

Table V. Analyte spike and recovery test in the three different sample types at six concentration levels

Sample type	Spiked (cg g ⁻¹)	Neodymium		Praseodymium		Iron		Boron	
		Found (cg g ⁻¹)	Rec (%)	Found (cg g ⁻¹)	Rec (%)	Found (cg g ⁻¹)	Rec (%)	Found (cg g ⁻¹)	Rec (%)
Didymium oxide	0.00	61.03 ± 0.23	***	25.04 ± 0.21	***	< MDL	***	< MDL	***
	0.05	61.08 ± 0.22	100	25.10 ± 0.18	120	< MDL	***	0.05 ± 0.03 ^a	100
	0.10	61.13 ± 0.25	100	25.14 ± 0.15	100	0.09 ± 0.04 ^a	90	0.10 ± 0.02	100
	0.50	61.52 ± 0.19	98	25.55 ± 0.12	102	0.49 ± 0.09	98	0.52 ± 0.04	104
	1.00	62.01 ± 0.31	98	26.08 ± 0.16	104	1.00 ± 0.15	100	0.99 ± 0.03	99
	1.50	62.55 ± 0.23	101	26.56 ± 0.22	101	1.49 ± 0.30	99	1.47 ± 0.12	98
	2.00	62.99 ± 0.26	98	27.05 ± 0.20	101	1.96 ± 0.48	98	2.02 ± 0.05	101
Metallic didymium	0.00	78.22 ± 0.33	***	22.41 ± 0.12	***	< MDL	***	< MDL	***
	0.05	78.28 ± 0.32	120	22.47 ± 0.11	120	< MDL	***	0.05 ± 0.02 ^a	100
	0.10	78.33 ± 0.35	110	22.53 ± 0.11	120	0.09 ± 0.05 ^a	90	0.10 ± 0.01	100
	0.50	78.74 ± 0.28	104	22.91 ± 0.16	100	0.48 ± 0.09	96	0.51 ± 0.03	102
	1.00	79.23 ± 0.22	101	23.44 ± 0.08	103	0.98 ± 0.12	98	1.01 ± 0.02	101
	1.50	79.75 ± 0.37	102	23.91 ± 0.22	100	1.53 ± 0.47	102	1.53 ± 0.07	102
	2.00	80.21 ± 0.34	99	24.43 ± 0.13	101	1.94 ± 0.57	97	1.98 ± 0.04	99
(Nd,Pr)-Fe-B alloy ^b	0.00	24.29 ± 0.07	***	6.59 ± 0.13	***	69.62 ± 0.83	***	1.07 ± 0.02	***
	0.05	24.34 ± 0.12	100	6.65 ± 0.03	120	69.69 ± 0.85	140	1.12 ± 0.01	100
	0.10	24.40 ± 0.10	110	6.70 ± 0.13	110	69.74 ± 0.94	120	1.17 ± 0.01	100
	0.50	24.78 ± 0.15	98	7.07 ± 0.14	96	70.14 ± 1.32	104	1.55 ± 0.09	96
	1.00	25.31 ± 0.13	102	7.62 ± 0.17	103	70.63 ± 0.97	101	2.06 ± 0.03	99
	1.50	25.77 ± 0.20	99	8.12 ± 0.16	102	71.16 ± 0.66	103	2.55 ± 0.02	99
	2.00	26.33 ± 0.16	102	8.63 ± 0.19	102	71.59 ± 1.05	98	3.11 ± 0.05	102

^aMass fraction value between MDL and PQL (MDL<x<PQL).^bSample analysed by different laboratories, shown in Table VI as "Sample C".

Table VI. Comparison of (Nd,Pr)-Fe-B alloy sample determinations and the conclusion of the student t-test at 95% confidence level

Sample	Element	Mass fraction (cg g ⁻¹)			Comparison					
		Guest Laboratory 1 ^a	Guest Laboratory 2 ^b	Proposed Method ^c	Student t-test		Statistically different ^d (t critical = 2.78)		Agreement ^f (%)	
					t _{LAB 1}	t _{LAB 2}	LAB 1	LAB 2	LAB 1	LAB 2
A	Nd	17.6 ± 0.9	17.2 ± 0.8	17.3 ± 0.3	0.55	0.20	Not	Not	102	99
	Pr	13.7 ± 0.7	14.0 ± 0.7	14.2 ± 0.4	1.07	0.43	Not	Not	96	99
	Fe	66.9 ± 3.3	not rated	67.0 ± 1.0	0.05	***	Not	***	100	***
	B	1.20 ± 0.06	1.04 ± 0.05	1.16 ± 0.03	1.03	3.56	Not	Yes	103	90
B	Nd	30.4 ± 1.5	30.4 ± 1.6	29.3 ± 0.3	1.25	1.17	Not	Not	104	104
	Pr	< 0.4 ^e	0.08 ± 0.01	0.07 ± 0.02	1.43	0.77	Not	Not	***	114
	Fe	68.0 ± 3.4	not rated	68.4 ± 1.7	0.18	***	Not	***	99	***
	B	1.10 ± 0.06	1.03 ± 0.05	1.03 ± 0.02	1.92	0.00	Not	Not	107	100
C	Nd	24.5 ± 1.2	24.5 ± 1.2	24.3 ± 1.3	0.20	0.20	Not	Not	101	101
	Pr	6.4 ± 0.3	6.3 ± 0.3	6.6 ± 0.4	0.69	1.04	Not	Not	97	95
	Fe	67.5 ± 3.3	not rated	69.6 ± 5.1	0.60	***	Not	***	97	***
	B	1.10 ± 0.06	0.91 ± 0.05	1.07 ± 0.06	0.61	3.55	Not	Yes	103	85

^aReported values based on ICP OES measurements.

^bReported values based on ICP-MS measurements, employing quadrupole as mass analyser.

^cMass fraction values reported by proposed method include the confidence interval with 5% of significance level.

^dHypothesis test: If t calculated > t critical, values are statistically different.

^eReported values < x, were considered x ± x for the student t-test calculation, ranging from non-existent in the sample (zero concentration) up to double the reported minimum detectable concentration limit.

^fAgreement calculated by (Guest laboratory result / Proposed method result) × 100

Foreign elements

Foreign chemical elements can be added to metal alloys to improve some specific characteristics for the application of permanent magnets,⁵¹ for example: Dysprosium (Dy) is usually added to the alloy composition aiming to increase the intrinsic coercivity at higher temperatures.³³ Other chemical elements can be added to the super-magnets such as: Nb,⁵¹ Ce,^{52,53} Tb,⁵⁴ Ga,^{55,56} Co,⁵⁷ Cu,^{53,58} La,⁵² Al,⁵⁸ among others. Usually, such elements have a low concentration, not exceeding 5 cg g⁻¹. As they have a different chemical nature from the analytes, it is possible that the foreign elements may interfere with the proposed analytical method. To assess the applicability of the proposed analytical method in the presence of foreign elements, mono-elemental standard solutions of 35 distinct chemical elements were analysed by ICP OES and the respective impacts on the analytical signals for the quantification of Nd, Pr, Fe and B were evaluated. The relative calibration sensitivity achieved for each foreign element at the monitored analytical lines (401.225, 414.311, 259.837 and 249.678 nm) is shown in Figure 3. The interference bias percentage values expressed in this figure correspond to the ratio between calibration sensitivity of foreign element and the calibration sensitivity of the analyte. As an example, a value of +10% interference bias caused by a foreign element in a given analyte makes each 1 cg g⁻¹ of the foreign element in the sample induces an error of about +0.1 cg g⁻¹ in the analyte quantification.

According to the results of Figure 3, the main interfering chemical elements in the neodymium quantification were: Cerium (+30.4%), europium (-6.4%), titanium (+2.9%), lutetium (+1.0 %) and samarium (-0.9%). In these specific cases of interference, alternative wavelengths can be used to quantify neodymium correctly, such as: 415.608 nm (good alternative to eliminate spectral interferences from Eu, Sm and Lu) or 406.109 nm (more suitable wavelength in the presence of cerium and titanium).

The determination of praseodymium was affected when present in the sample: Dysprosium (+13.5%), molybdenum (-6.3%), terbium (-2.5%) and niobium (+1.3%), with alternatives for a reliable measurement of praseodymium at 422.293 nm (aiming to eliminate the interferences from Dy and Mo) or at 422.535 nm (excellent to avoid spectral interference from Tb and Nb).

The iron characteristic wavelength (259.837 nm) can suffer interference from tantalum (+1.8%) and gold (+1.3%), a possible line free from these interferences corresponds to 238.204 nm. However, it is worth mentioning that in metallic alloys the impact of interference in the quantification of iron will be minimal, since iron is normally a component present in high concentrations in metallic alloys, being considered the “diluent” of the alloys, reaching concentrations of up to 70 cg g⁻¹, and in this concentration level the error induced by the spectral interference will not be significant.

In the interference evaluation, the quantification of boron was affected only by hafnium (-1.4%). In this case, a plausible alternative consists in measure boron at 182.641 nm. The other elements (Al, Ca, Co, Cr, Cu, Er, Ga, Gd, Ho, K, La, Li, Mg, Mn, Nb, Pb, Sc, Si, Sn, Tm, V, Yb, Zn and Zr) did not exhibit significant interference and therefore do not affect the applicability of this proposed analytical method.

Any spectral interferences that result in a negative bias are explained by optical emissions in regions close to those selected for the background calculation. Similarly, the interferences that result in a positive bias come from optical emissions that occur close to the central pixel.

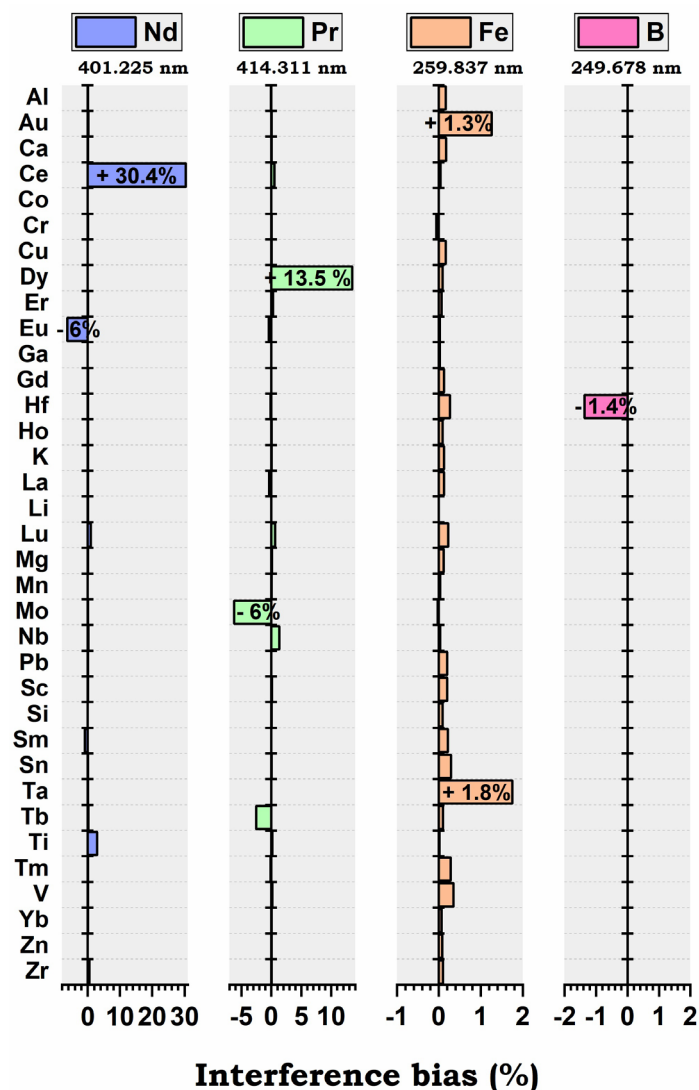


Figure 3. Interference chart showing the impact of foreign chemical elements in the calibration sensitivity of Nd, Pr, Fe and B in the proposed analytical method. The interference bias percentage value was calculated by the calibration sensitivity of the foreign element (estimated from two concentrations: 1 and 10 mg L⁻¹) divided by calibration sensitivity of the analyte.

Comparative analytical methods, advantages and drawbacks

Determinations of Nd, Pr, Fe and B in the samples related to the production chain of the permanent magnets have been explored by places that contain natural reserves of rare earth elements and that consequently dominate the production technology of super-magnets. The main publications related to this topic are concentrated in China, a country that exploits rare earth elements. Although many studies use chemical analysis to characterize samples related to the production process of super-magnets, few articles detail the methods and its figures of merit, parameters that are essential to compare and select an appropriate analytical method. Therefore, the scarcity of studies dedicated to the rigorous chemical analysis of these materials in the scientific literature hinders the comparison with other analytical methods. In this section, the proposed method was compared with another analytical methods that have at least one similar matrix or similar analytes that demonstrate a rigorous development. A summary comparison of the methods is shown in Table VII.

Two different studies stand out for minimizing sample preparation, proposing a direct analysis of magnets in hard disk devices (HD) by WD-XRF⁵⁹ and LIBS.⁶⁰ Although such methods have indisputable advantages when compared to the proposed method in this paper (that requires sample dissolution), the quantification of Nd by WD-XRF shown interference from Pr.⁵⁹ Such interference was not a problem in the

samples evaluated in the mentioned study, since the concentrations of Pr were lower than the 5 cg g^{-1} ,⁵⁹ but this is a different reality from that found in the samples related to the production process of didymium magnets, whose levels of Pr reached up to 25 cg g^{-1} . Therefore, the interference is a problem of that could lead to inadequate results when applied to didymium samples. In addition, both mentioned studies needed to know reference values of the analytes in samples for a suitable calibration, requiring to quantify the elements from the dissolved samples by ICP OES.^{59,60}

The elemental analysis in HD magnets by ICP OES was proposed by Castro *et al.*⁶¹ This important work reports, for the first time, a detailed method of chemical analysis of magnets by wet dissolution, with other conditions. When compared, the current work stands out: (i) for the application in different types of samples, (ii) for the rigorous studies of precision and accuracy and (iii) for the study of interference that allows a wide scope of application of this method. Differentials that highlight this work as an important reference in the scientific literature, establishing a standard method for the chemical analysis of magnets composed of neodymium and praseodymium.

Proposed by Papai *et al.*³ the determination of Nd and Pr was successfully performed in samples of metallic didymium and (Nd, Pr)-Fe-B alloy, standing out for employing low resolution atomic emission spectrometry with a flame composed of acetylene/nitrous oxide and a mathematical approach to solve the spectral interferences. Although this method uses a more accessible spectrometer and less expensive cost of analysis when compared to the proposed method in this paper, it has a greater susceptibility to spectral interference from other elements, requiring mono-elemental calibrations and a suitable mathematical approach before providing the results. Furthermore, only the quantification of the elements Nd and Pr is performed, in contrast to the simultaneous quantification of four elements (Nd, Pr, Fe, B) in the proposed method.

Thus, the main advantages of the proposed method are: (i) simultaneous determination of Nd, Pr, Fe and B; (ii) versatility for application in different sample types related to the production process of super-magnets; (iii) high reliability of the results; (iv) low susceptibility to spectral interferences with alternatives to avoid them completely and (v) low uncertainties provided by triplicate ($n = 3$).

The main drawbacks to this method are: (i) the need to dissolve samples in an acid medium, whereas a faster quantification could be obtained by direct analysis of solids techniques; (ii) cost of analysis, since the consumption of argon has a significant impact on the laboratory's budget and (iii) the need to weigh all dilution steps, which requires more time from the analyst. Despite these drawbacks, the method clearly meets the needs for strict chemical quality control.

Table VII. Comparison of the current method with others reported in the scientific literature

Analytes	Sample type	Instrumental technique	Sample treatment	Advantages	Drawbacks	Ref.
Nd and Pr	(Nd,Pr)-Fe-B alloy Metallic Didymium	F AES ^a	Acidic dissolution (HNO ₃ and HCl)	*Accessible spectrometer; *Low-cost; *Fast analysis	*Susceptibility to spectral interference; *Need unusual math approach to quantify	(3)
Nd	Hard Disk magnets	WD-XRF ^b	None or minimal	*Direct solid analysis; *Non-destructive; *Fast analysis;	*Subject to Pr interference;	(59)
Nd, Pr, Fe, B and others	Hard Disk magnets	LIBS ^c	None or minimal	*Direct solid analysis; *Fast acquisition of complete spectra;	*Calibration (need for samples with known reference values)	(60)
Nd, Pr, Fe, B and others	Hard Disk magnets	ICP OES	Acidic dissolution (HNO ₃ and HCl)	*Simultaneous determination	*Need sample dissolution; *Cost of analysis;	(61)
Nd, Pr, Fe and B	(Nd,Pr)-Fe-B alloy Metallic Didymium Didymium oxide	ICP OES	Acidic dissolution (HNO ₃ and HCl)	*Simultaneous determination; *High reliability; *Strict and high precision results guaranteed *Low susceptibility to spectral interferences; *Foreign elements evaluation;	*Need sample dissolution; *Cost of analysis;	This work

^aFlame Atomic Emission Spectrometry

^bWavelength dispersive X-ray Fluorescence

^cLaser-Induced Breakdown Spectrometry

CONCLUSIONS AND OUTLOOKS

The proposed method provided high precision results, with good accuracy and fulfilled the purpose of the strict quality control of the permanent magnets materials, solving the pressing need to distinguish neodymium and praseodymium concentrations in less than 1 cg g^{-1} .

The control of the dilution steps by weighing proved to be essential to achieve the low values of uncertainty reported in Table IV. Despite the weighing procedure adding an additional step in the proposed analytical method, that requires the most time from the analyst, this characteristic should not be considered a resistance to routine implementation, since there is a significant gain in improving precision and consequently reliability. This gain in reliability is associated with an improvement in the quality and performance of the final products since the chemical control throughout the production process impacts and guides the production routes to obtain materials within the required specifications.

The method was shown to be versatile, being easily applicable to at least three different sample types (didymium oxide, metallic didymium and (Nd,Pr)-Fe-B alloys).

The analytical method proved to be robust with few potentially interfering foreign elements. In the few verified cases of possible interference, alternative wavelengths have been suggested that eliminate spectral interferences.

As a perspective, this reported method paves the way for the production of standard materials to be applied in other instrumental techniques aimed at direct analysis of solids.

Conflicts of interest

The authors declare that they have no known competing financial interests or personal relationships that could have appeared to influence the work reported in this paper.

Acknowledgements

Funding sources: (i) “Conselho Nacional de Desenvolvimento Científico e Tecnológico” (CNPq) [465719/2014-7]; (ii) “Coordenação de Aperfeiçoamento de Pessoal de Nível Superior” (CAPES) [23038000776/2017-54]; (iii) “Fundação de Amparo à Pesquisa do Estado de São Paulo” (FAPESP) [2014/50887-4] and (iv) “Banco Nacional do Desenvolvimento” (BNDES FUNTEC).

Fellowships granted to: Rodrigo Papai (CNPq) [380490/2018-8] and [380939/2020-7], and Thiago Pires Nagasima (CNPq) [381315/2017-7].

The authors are also grateful to Bruno Menezes Siqueira (Product Manager and Application Scientist, M.Sc) for initial training in ICP OES instrument, Valeska Meirelles (Field Service Engineer and Application Scientist, Ph.D) for quick assistance, Tiago Finatte (Field Service Engineer) for technical support and Nova Analítica company for kindly granting an ICP OES instrument (iCap 7400) for use in our laboratory.

REFERENCES

- (1) Dent, P. C. Rare earth elements and permanent magnets. *J. Appl. Phys.* **2012**, *111* (7), 07A721. <https://doi.org/10.1063/1.3676616>
- (2) Nicola, J. Materials science: The pull of stronger magnets. *Nature* **2011**, *472* (7341), 22-23. <https://doi.org/10.1038/472022a>
- (3) Papai, R.; de Freitas, M. A. S.; da Fonseca, K. T.; de Almeida, G. A.; da Silveira, J. R. F.; da Silva, A. L. N.; Ferreira Neto, J. B.; dos Santos, C. A. L.; Landgraf, F. J. G.; Luz, M. S. Additivity of optical emissions applied to neodymium and praseodymium quantification in metallic didymium and (Nd,Pr)-Fe-B alloy samples by low-resolution atomic emission spectrometry: An evaluation of the mathematical approach used to solve spectral interferences. *Anal. Chim. Acta* **2019**, *1085*, 21-28. <https://doi.org/10.1016/j.aca.2019.07.049>
- (4) Li, J.; Huang, X.; Zeng, L.; Ouyang, B.; Yu, X.; Yang, M.; Yang, B.; Rawat, R. S.; Zhong, Z. Tuning magnetic properties, thermal stability and microstructure of NdFeB magnets with diffusing Pr-Zn films. *J. Mater. Sci. Technol.* **2020**, *41*, 81-87. <https://doi.org/10.1016/j.jmst.2019.09.024>

- (5) Rehman, S. U.; Jiang, Q.; He, L.; Xiong, H.; Liu, K.; Wang, L.; Yang, M.; Zhong, Z. Microstructure and magnetic properties of NdFeB alloys by co-doping alnico elements. *Phys. Lett. A* **2019**, *383* (31), 125878. <https://doi.org/10.1016/j.physleta.2019.125878>
- (6) Jiang, Q.; He, L.; Rehman, S. U.; Hu, Y.; Song, J.; Ouyang, H.; Yang, M.; Zhong, Z. Optimized composition and improved magnetic properties of Ce-Fe-B alloys. *J. Alloys Compd.* **2019**, *811*, 151998. <https://doi.org/10.1016/j.jallcom.2019.151998>
- (7) Xu, X. D.; Dong, Z. J.; Sasaki, T. T.; Tang, X.; Sepehri-Amin, H.; Ohkubo, T.; Hono, K. Influence of Ti addition on microstructure and magnetic properties of a heavy-rare-earth-free Nd-Fe-B sintered magnet. *J. Alloys Compd.* **2019**, *806*, 1267-1275. <https://doi.org/10.1016/j.jallcom.2019.07.289>
- (8) Mackie, A. J.; Dean, J. S.; Goodall, R. Material and magnetic properties of $\text{Sm}_2(\text{Co}, \text{Fe}, \text{Cu}, \text{Zr})_{17}$ permanent magnets processed by Spark Plasma Sintering. *J. Alloys Compd.* **2019**, *770*, 765-770. <https://doi.org/10.1016/j.jallcom.2018.08.186>
- (9) Jiang, Q.; Zhong, Z. Research and development of Ce-containing $\text{Nd}_2\text{Fe}_{14}\text{B}$ -type alloys and permanent magnetic materials. *J. Mater. Sci. Technol.* **2017**, *33* (10), 1087-1096. <https://doi.org/10.1016/j.jmst.2017.06.019>
- (10) Zeng, H. X.; Liu, Z. W.; Zhang, J. S.; Liao, X. F.; Yu, H. Y. Towards the diffusion source cost reduction for NdFeB grain boundary diffusion process. *J. Mater. Sci. Technol.* **2020**, *36*, 50-54. <https://doi.org/10.1016/j.jmst.2019.08.009>
- (11) Engerhoff, J. A. B.; Baldissera, A. B.; Magalhães, M. D.; Lamarão, P. H.; Wendhausen, P. A. P.; Ahrens, C. H.; Mascheroni, J. M. Additive manufacturing of Sm-Fe-N magnets. *J. Rare Earths* **2019**, *37* (10), 1078-1082. <https://doi.org/10.1016/j.jre.2019.04.012>
- (12) Thornton, B. F.; Burdette, S. C. The neodymium neologism. *Nat. Chem.* **2017**, *9*, 194. <https://doi.org/10.1038/nchem.2722>
- (13) Dingle, A. Praseodymium unpaired. *Nat. Chem.* **2018**, *10* (5), 576-576. <https://doi.org/10.1038/s41557-018-0050-7>
- (14) Fim, R. G. T.; Mascheroni, A. A.; Antunes, L. F.; Engerhoff, J. B. E.; Ahrens, C. H.; Wendhausen, P. A. P. Increasing packing density of Additively Manufactured Nd-Fe-B bonded magnets. *Addit. Manuf.* **2020**, *35*, 101353. <https://doi.org/10.1016/j.addma.2020.101353>
- (15) Liu, Y.; Xia, W.; Liu, J. P.; Du, J.; Yan, A.; Guan, D.; Liu, Y.; Zhang, J. Coercivity enhancement and mechanism in a high Ce-containing Nd-Ce-Fe-B film by the design of a diffusion layer. *J. Mater. Chem. C* **2019**, *7* (24), 7318-7326. <https://doi.org/10.1039/C9TC01279F>
- (16) Rollat, A.; Guyonnet, D.; Planchon, M.; Tuduri, J. Prospective analysis of the flows of certain rare earths in Europe at the 2020 horizon. *Waste Management* **2016**, *49*, 427-436. <https://doi.org/10.1016/j.wasman.2016.01.011>
- (17) München, D. D.; Veit, H. M. Neodymium as the main feature of permanent magnets from hard disk drives (HDDs). *Waste Management* **2017**, *61*, 372-376. <https://doi.org/10.1016/j.wasman.2017.01.032>
- (18) Pathak, A. K.; Gschneidner, K. A.; Khan, M.; McCallum, R. W.; Pecharsky, V. K. High performance Nd-Fe-B permanent magnets without critical elements. *J. Alloys Compd.* **2016**, *668*, 80-86. <https://doi.org/10.1016/j.jallcom.2016.01.194>
- (19) Yang, F.; Zhang, X.; Guo, Z.; Ye, S.; Sui, Y.; Volinsky, A. A. 3D printing of NdFeB bonded magnets with $\text{SrFe}_{12}\text{O}_{19}$ addition. *J. Alloys Compd.* **2019**, *779*, 900-907. <https://doi.org/10.1016/j.jallcom.2018.11.335>
- (20) Yuping, L.; Mengling, W.; Jiayu, L. Sintered Nd-Fe-B magnet with core-shell structures fabricated through the intergranular addition of ultra-fine as-disproportionated (Nd,Dy)-Fe-B-Cu powder. *J. Mater. Sci.: Mater. Electron.* **2020**, *31* (9), 7211-7218. <https://doi.org/10.1007/s10854-020-03293-y>
- (21) Ma, B.; Bao, X.; Sun, A.; Li, J.; Cao, S.; Gao, X.-x. Normal and Abnormal Grain Growth in Hydrogenation-Disproportionation-Desorption-Recombination Processed Nd-Fe-B Strip-Cast Alloys. *Cryst. Growth Des.* **2020**, *20* (5), 3119-3130. <https://doi.org/10.1021/acs.cgd.0c00006>

- (22) Ikram, A.; Mehmood, F.; Sheridan, R. S.; Awais, M.; Walton, A.; Eldosouky, A.; Sturm, S.; Kobe, S.; Rozman, K. Z. Particle size dependent sinterability and magnetic properties of recycled HDDR Nd–Fe–B powders consolidated with spark plasma sintering. *J. Rare Earths* **2020**, *38* (1), 90-99. <https://doi.org/10.1016/j.jre.2019.02.010>
- (23) Fim, R. G. T.; Silva, M. R. M.; Silva, S. C.; Casini, J. C. S.; Wendhausen, P. A. P.; Takiishi, H. Influence of Milling Time on Magnetic Properties and Microstructure of Sintered Nd-Fe-B Based Permanent Magnets. *Mater. Sci. Forum* **2018**, *930* 445-448. <https://doi.org/10.4028/www.scientific.net/MSF.930.445>
- (24) Kianvash, A.; Harris, I. R. The influence of free iron on the hydrogen decrepitation capability of some Nd(Pr)–Fe–B alloys. *J. Alloys Compd.* **1998**, *279* (2), 245-251. [https://doi.org/10.1016/S0925-8388\(98\)00652-5](https://doi.org/10.1016/S0925-8388(98)00652-5)
- (25) Machado, R. C.; Andrade, D. F.; Babos, D. V.; Castro, J. P.; Costa, V. C.; Sperança, M. A.; Garcia, J. A.; Gamela, R. R.; Pereira-Filho, E. R. Solid sampling: advantages and challenges for chemical element determination—a critical review. *J. Anal. At. Spectrom.* **2020**, *35*, 54-77. <https://doi.org/10.1039/C9JA00306A>
- (26) Costa, V. C.; Castro, J. P.; Andrade, D. F.; Babos, D. V.; Garcia, J. A.; Sperança, M. A.; Catelani, T. A.; Pereira-Filho, E. R. Laser-induced breakdown spectroscopy (LIBS) applications in the chemical analysis of waste electrical and electronic equipment (WEEE). *TrAC, Trends Anal. Chem.* **2018**, *108*, 65-73. <https://doi.org/10.1016/j.trac.2018.08.003>
- (27) Papai, R.; Mariano, C. S.; Pereira, C. V.; da Costa, P. V. F.; Leme, F. O.; Nomura, C. S.; Gaubeur, I. Matte photographic paper as a low-cost material for metal ion retention and elemental measurements with laser-induced breakdown spectroscopy. *Talanta* **2019**, *205*, 120167. <https://doi.org/10.1016/j.talanta.2019.120167>
- (28) Noll, R.; Fricke-Begemann, C.; Connemann, S.; Meinhardt, C.; Sturm, V. LIBS analyses for industrial applications – an overview of developments from 2014 to 2018. *J. Anal. At. Spectrom.* **2018**, *33* (6), 945-956. <https://doi.org/10.1039/C8JA00076J>
- (29) Papai, R.; Sato, R. H.; Nunes, L. C.; Krug, F. J.; Gaubeur, I. Melted Paraffin Wax as an Innovative Liquid and Solid Extractant for Elemental Analysis by Laser-Induced Breakdown Spectroscopy. *Anal. Chem.* **2017**, *89* (5), 2807-2815. <https://doi.org/10.1021/acs.analchem.6b03766>
- (30) Fortes, F. J.; Moros, J.; Lucena, P.; Cabalín, L. M.; Laserna, J. J. Laser-Induced Breakdown Spectroscopy. *Anal. Chem.* **2013**, *85* (2), 640-669. <https://doi.org/10.1021/ac303220r>
- (31) Vanhoof, C.; Bacon, J. R.; Ellis, A. T.; Vincze, L.; Wobrauschek, P. 2018 atomic spectrometry update – a review of advances in X-ray fluorescence spectrometry and its special applications. *J. Anal. At. Spectrom.* **2018**, *33* (9), 1413-1431. <https://doi.org/10.1039/C8JA90030B>
- (32) Vanhoof, C.; Bacon, J. R.; Ellis, A. T.; Fittschen, U. E. A.; Vincze, L. 2019 atomic spectrometry update – a review of advances in X-ray fluorescence spectrometry and its special applications. *J. Anal. At. Spectrom.* **2019**, *34* (9), 1750-1767. <https://doi.org/10.1039/C9JA90042J>
- (33) Imashuku, S.; Takahashi, J.; Kunimura, S.; Wagatsuma, K. Application of Portable Total-Reflection X-Ray Fluorescence Spectrometer to Analysis of Dysprosium in Neodymium-Iron-Boron Magnet. *ISIJ Int.*, **2016**, *56* (12), 2224-2227. <https://doi.org/10.2355/isijinternational.ISIJINT-2016-349>
- (34) Russo, R. E.; Mao, X.; Gonzalez, J. J.; Zorba, V.; Yoo, J. Laser Ablation in Analytical Chemistry. *Anal. Chem.* **2013**, *85* (13), 6162-6177. <https://doi.org/10.1021/ac4005327>
- (35) Augusto, A. S.; Sperança, M. A.; Andrade, D. F.; Pereira-Filho, E. R. Nutrient and Contaminant Quantification in Solid and Liquid Food Samples Using Laser-Ablation Inductively Coupled Plasma-Mass Spectrometry (LA-ICP-MS): Discussion of Calibration Strategies. *Food Analytical Methods* **2017**, *10* (5), 1515-1522. <https://doi.org/10.1007/s12161-016-0703-3>
- (36) Alonso, E. V.; Guerrero, M. M. L.; Cordero, M. T. S.; Pavón, J. M. C.; de Torres, A. G. Characterization of solid magnetic nanoparticles by means of solid sampling high resolution continuum source electrothermal atomic absorption spectrometry. *J. Anal. At. Spectrom.* **2016**, *31* (12), 2391-2398. <https://doi.org/10.1039/C6JA00225K>

- (37) Leme, F. O.; Lima, L. C.; Papai, R.; Akiba, N.; Batista, B. L.; Gaubeur, I. A novel vortex-assisted dispersive liquid-phase microextraction procedure for preconcentration of europium, gadolinium, lanthanum, neodymium, and ytterbium from water combined with ICP techniques. *J. Anal. At. Spectrom.* **2018**, *33* (11), 2000-2007. <https://doi.org/10.1039/C8JA00252E>
- (38) Zawisza, B.; Pytlakowska, K.; Feist, B.; Polowniak, M.; Kita, A.; Sitko, R. Determination of rare earth elements by spectroscopic techniques: a review. *J. Anal. At. Spectrom.* **2011**, *26* (12), 2373-2390. <https://doi.org/10.1039/C1JA10140D>
- (39) Renko, M.; Osojnik, A.; Hudnik, V. ICP emission spectrometric analysis of rare earth elements in permanent magnet alloys. *Fresenius' Journal of Analytical Chemistry* **1995**, *351* (7), 610-613. <https://doi.org/10.1007/BF00323334>
- (40) Santos, C. A.; Panossian, Z. Permanent Rare-Earth Magnets – The need to protect them against corrosion. *Materials Sciences and Applications* **2019**, *10*, 317-327. <https://doi.org/10.4236/msa.2019.104024>
- (41) Carter, J. A.; Barros, A. I.; Nóbrega, J. A.; Donati, G. L. Traditional Calibration Methods in Atomic Spectrometry and New Calibration Strategies for Inductively Coupled Plasma Mass Spectrometry. *Frontiers in Chemistry* **2018**, *6* (504). <https://doi.org/10.3389/fchem.2018.00504>
- (42) Virgilio, A.; Gonçalves, D. A.; McSweeney, T.; Gomes Neto, J. A.; Nóbrega, J. A.; Donati, G. L. Multi-energy calibration applied to atomic spectrometry. *Anal. Chim. Acta* **2017**, *982*, 31-36. <https://doi.org/10.1016/j.aca.2017.06.040>
- (43) Williams, C. B.; Jones, B. T.; Donati, G. L. Multi-flow calibration applied to microwave-induced plasma optical emission spectrometry. *J. Anal. At. Spectrom.* **2019**, *34* (6), 1191-1197. <https://doi.org/10.1039/C9JA00091G>
- (44) Donati, G. L.; Amais, R. S. Fundamentals and new approaches to calibration in atomic spectrometry. *J. Anal. At. Spectrom.* **2019**, *34*, 2353-2369. <https://doi.org/10.1039/C9JA00273A>
- (45) Ingle Jr, J. D.; Crouch, S. R. *Spectrochemical Analysis*, Prentice Hall, Upper Saddle River, New Jersey, United States, **1988**.
- (46) ASTM E456-13ae4 *Standard Terminology Relating to Quality and Statistics*, ASTM International, West Conshohocken, PA, **2013**.
- (47) ASTM E177-14 *Standard Practice for Use of the Terms Precision and Bias in ASTM Test Methods*, ASTM International, West Conshohocken, PA, **2014**.
- (48) Thompson, M. Variation of precision with concentration in an analytical system. *Analyst* **1988**, *113* (10), 1579-1587. <https://doi.org/10.1039/AN9881301579>
- (49) Horwitz, W. Evaluation of analytical methods used for regulation of foods and drugs. *Anal. Chem.* **1982**, *54* (1), 67-76. <https://doi.org/10.1021/ac00238a002>
- (50) Horwitz, W.; Albert, R. Precision in analytical measurements: Expected values and consequences in geochemical analyses. *Fresenius' Journal of Analytical Chemistry*, **1995**, *351* (6), 507-513. <https://doi.org/10.1007/bf00322724>
- (51) da Silva, M. R. M.; Fim, R. G. T.; Silva, S. C.; Casini, J. C. S.; Wendhausen, P. A. P.; Takiishi, H. Influence of Alloying Elements Zr, Nb and Mo on the Microstructure and Magnetic Properties of Sintered Pr-Fe-Co-B Based Permanent Magnets. *Mater. Sci. Forum*, **2018**, *930*, 440-444. <https://doi.org/10.4028/www.scientific.net/MSF.930.440>
- (52) Jin, J.; Yan, M.; Ma, T.; Li, W.; Liu, Y.; Zhang, Z.; Fu, S. Balancing the microstructure and chemical heterogeneity of multi-main-phase Nd-Ce-La-Fe-B sintered magnets by tailoring the liquid-phase-sintering. *Materials & Design* **2020**, *186*, 108308. <https://doi.org/10.1016/j.matdes.2019.108308>
- (53) Cui, X. G.; Zhang, H. J.; Pan, J. X.; Cui, C. Y.; Cheng, L. L.; Ma, T. Y.; Zhang, J.; Wang, C.; Chen, T. H.; Xu, X. J. Magnetic properties, thermal stability, and microstructure of spark plasma sintered multi-main-phase Nd-Ce-Fe-B magnet with PrCu addition. *J. Alloys Compd.* **2020**, *822*, 153612. <https://doi.org/10.1016/j.jallcom.2019.153612>

- (54) Skotnicova, K.; Burkhanov, G. S.; Kolchugina, N. B.; Kursa, M.; Cegan, T.; Lukin, A. A.; Zivotsky, O.; Prokofev, P. A.; Jurica, J.; Li, Y. Structural and magnetic engineering of (Nd, Pr, Dy, Tb)–Fe–B sintered magnets with Tb₃Co_{0.6}Cu_{0.4}Hx composition in the powder mixture. *J. Magn. Magn. Mater.* **2020**, *498*, 166220. <https://doi.org/10.1016/j.jmmm.2019.166220>
- (55) Li, J.; Tang, X.; Sepehri-Amin, H.; Sasaki, T. T.; Ohkubo, T.; Hono, K. Angular dependence and thermal stability of coercivity of Nd-rich Ga-doped Nd–Fe–B sintered magnet. *Acta Mater.* **2020**, *187*, 66-72. <https://doi.org/10.1016/j.actamat.2020.01.035>
- (56) Cho, Y.; Sasaki, T.; Harada, K.; Sato, A.; Tamaoka, T.; Shindo, D.; Ohkubo, T.; Hono, K.; Murakami, Y. Magnetic flux density measurements from grain boundary phase in 0.1 at% Ga-doped Nd–Fe–B sintered magnet. *Scr. Mater.* **2020**, *178*, 533-538. <https://doi.org/10.1016/j.scriptamat.2019.12.030>
- (57) Rezchikova, I. I.; Moiseeva, N. S.; Valeev, R. A.; Morgunov, R. B.; Piskorskii, V. P. Change in the Magnetization of Sintered Pr–Dy–Fe–Co–B Magnets in Time. *Russ. Metall.* **2020**, 66-70. <https://doi.org/10.1134/S0036029520010097>
- (58) Lu, K.; Bao, X.; Zhou, Y.; Lv, X.; Ding, Y.; Zhang, M.; Wang, C.; Gao, X. Effect of Al/Cu on the magnetic properties and microstructure of Nd-Fe-B sintered magnet by diffusing Pr-Tb-(Cu, Al) alloys. *J. Magn. Magn. Mater.* **2020**, *500*, 166384. <https://doi.org/10.1016/j.jmmm.2019.166384>
- (59) Castro, J. P.; Sperança, M. A.; Babos, D. V.; Andrade, D. F.; Pereira-Filho, E. R. Neodymium determination in hard drive disks magnets using different calibration approaches for wavelength dispersive X-ray fluorescence. *Spectrochim Acta B* **2020**, *164*, 105763. <https://doi.org/10.1016/j.sab.2019.105763>
- (60) Castro, J. P.; Babos, D. V.; Pereira-Filho E. R., Calibration strategies for the direct determination of rare earth elements in hard disk magnets using laser-induced breakdown spectroscopy. *Talanta* **2020**, *208*, 120443. <https://doi.org/10.1016/j.talanta.2019.120443>
- (61) Castro, J. P.; Pereira-Filho, E. R. Spectroanalytical method for evaluating the technological elements composition of magnets from computer hard disks. *Talanta* **2018**, *189*, 205-210. <https://doi.org/10.1016/j.talanta.2018.06.062>